CrystEngComm

Accepted Manuscript

ROYAL SOCIETY OF CHEMISTRY

www.rsc.org/crystengcomm

Cite this: DOI: 10.1039/c0xx00000x

www.rsc.org/xxxxxx

PAPER

A topotactic transition in a liquid crystal compound†

Roberto Centore,*[a] Valeria Capitolino,[a] Francesca Cerciello,[b] Angela Tuzi,[a] Fabio Borbone,[a] Antonio Carella[a] and Antonio Roviello[a]

Received (in XXX, XXX) Xth XXXXXXXXX 201X, Accepted Xth XXXXXXXXX 201X

DOI: 10.1039/b000000x

The title compound, bis(4-butyloxyacetophenon)azine, exhibits a rich phase behavior. It has two different crystal phases and one liquid crystal phase before the transition to the isotropic liquid. The liquid crystalline phase is nematic. All the phase transitions of the compound are reversible. In particular, the solid-solid transition at 83 °C is single-crystal-to-single-crystal as proven by optical and electron microscopy and X-ray diffraction analysis and it shows a remarkable degree of reversibility: single crystals can undergo several cycles of transitions between the two phases without any damage. The crystal phase stable at lower temperature has been fully characterized by single crystal X-ray analysis. It shows an arrangement of the molecules in layers in the plane (a, b), with the layers piled up along c without interdigitation of the alkyl tails of molecules belonging to consecutive layers. The crystal phase stable at higher temperature is disordered.

Introduction

Polymorphism discloses challenging problems in crystallography.[1] The occurrence of different crystal forms for the same chemical substance was early observed in pure elements and minerals,[2] often crystallizing in high symmetry space groups. With the progress of the structural information it was also found in organics, so that it can be considered an intrinsic feature of the solid state. Here comes the first challenging problem about polymorphism: does every compound has more than one crystal form? And, if yes, how many different crystalline forms can be obtained for a given compound?[1,3]

Polymorphism can be classified in different ways. Thermotropic polymorphism means that the different polymorphs are obtained by action of temperature (*i. e.* by heating or cooling). In other cases, different crystal phases can be obtained by action of solvents.[4] If the transition from one form to the other is reversible, the polymorphism is classified as enantiotropic, if it is not, the polymorphism is named monotropic. A classification of polymorphism based on morphological features leads to the concept of topotaxy.[5] In a topotactic transition there is a well defined relation between the orientation of the crystal axes before and after the transition.[6] If that relation is a one-to-one correspondence, the transition transforms a single crystal of one polymorph into a single crystal of the other polymorph, *i. e.* it is a single-crystal-to-single-crystal transition (hereafter SCSC transition). Topotactic transitions are rare. In most cases of solid state polymorphism, there is no relation between the orientation of the crystal axes before and after the transition, so a single crystal of one polymorph is transformed in a mosaic of very small single crystals of the other polymorph randomly oriented with respect to each other, and the corresponding diffraction pattern is completely analogous to that produced by a powder sample. Actually, topotactic transitions are unique, because in these transitions the movement of microscopic individuals (atoms, molecules) is strongly correlated in space (and time) over macroscopic distances. An additional, intriguing feature sporadically observed in SCSC transitions is the thermosalient effect:[7] during the transition, single crystals undergo jumps and leaps over distances greater than crystal's dimensions. Both topotacticity and thermosalient effect are challenging problems in crystallography. It is not presently known what conditions must be met in order to have a SCSC transition and, within this, to have a thermosalient transition.

In the present paper we report on a case of SCSC transition in the compound bis(4-butyloxyacetophenon)azine, hereafter C4F3, whose chemical diagram is shown in Scheme 1.

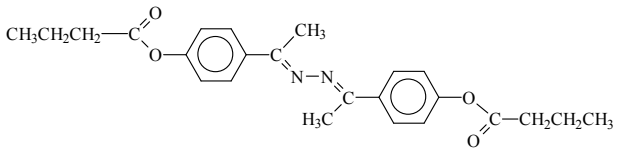

Scheme 1 Chemical diagram of the studied compound.

This compound was synthesized several years ago, together with similar compounds having terminal chains of different length,[8] as model compounds of liquid-crystalline polymers.[9] In the original paper[8] it was only stated, based on polarizing microscopy, that C4F3 undergoes a topotactic transition. Here we report a complete characterization of the transition based on optical and elctron microscopy, thermodynamic measurements and structural analysis.

Results and discussion

Thermodynamic, optical and electron microscopy characterization

C4F3 exhibits a rich phase behaviour, as evidenced by the DSC thermograms reported in Fig. 1. There is an enantiotropic solid state transition at 83 °C (ΔH = 8.74 kJ/mol). Melting is at 121 °C (ΔH = 20.30 kJ/mol) with formation of a liquid crystalline (LC) phase having a fair interval of stability. The liquid crystal phase transforms in the isotropic liquid (IL) at 160 °C through a first order transition (ΔH = 0.90 kJ/mol). As it is evident from Fig. 1, all the phase transitions of C4F3 are reversible and show thermal hysteresis.

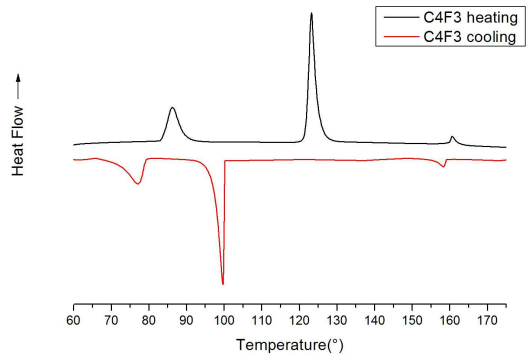

Fig. 1 DCS thermograms of C4F3 on heating and cooling. Scanning rate 10 K/min.

We note, from Fig. 1, the small supercooling of the IL to LC transition (about 1 °C) and of the solid-solid transition (about 3 °C) as compared with the LC to crystal transition that supercools considerably (about 21 °C).[10] The liquid crystal phase was identified as nematic.[8] In Fig. 2 we report the thread-like texture of the liquid crystal phase, which is compatible with a nematic liquid crystal phase.[11]

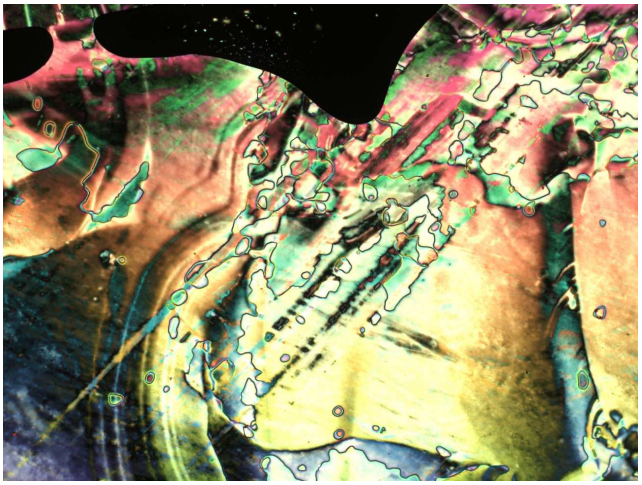

Fig. 2 Texture of the liquid crystal phase of C4F3 observed at 135 °C (crossed polarizers). Magnification factor 50x.

The solid state transition at 87 °C is a SCSC transition. In Fig. 3 a single crystal of C4F3, in the form of a thin lozenge, is photographed at the polarizing microscope under crossed polarizers at 70 °C (crystal phase I), at 95 °C, after the transition to the crystal phase II, and then again at 70 °C after the reverse transition to phase I has occurred: only a reversible change of interference colours is observed at the transition. No large variation is observed in the shape and dimensions of the crystal, and this can suggest that the structural variations associated with the solid state transition are small.

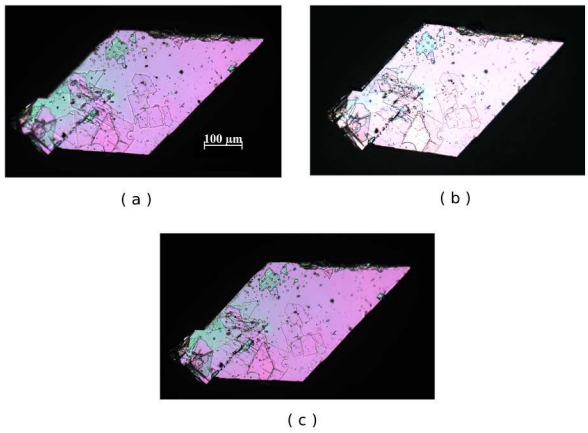

Fig. 3 (a) One single crystal of C4F3 at 70 °C, crossed polarizers; (b) the same crystal at 95 °C after the solid-solid transition, crossed polarizers; (c) the same crystal again at 70 °C after cooling from (b), crossed polarizers.

Single crystals as that of Fig. 3 can be subjected to many consecutive cycles of transitions between phases I and II without any damage. In Fig. 4 are reported SEM images of a single crystal of C4F3 never subjected to the solid state transition, while in Fig. 5 are reported SEM images of a single crystal from the same batch, after five consecutive cycles of transitions between phases I and II. The images are taken at room temperature.

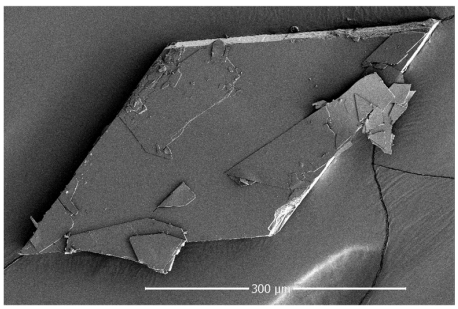

(a)

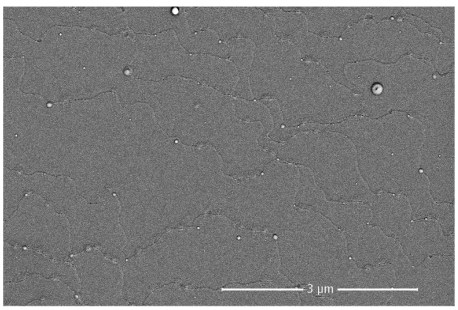

(b)

Fig. 4 (a) SEM images of a lozenge crystal of C4F3 as prepared. The scale bar is 300 μm. (b) SEM image of a portion of the surface of the lozenge. The scale bar is 3 μm.

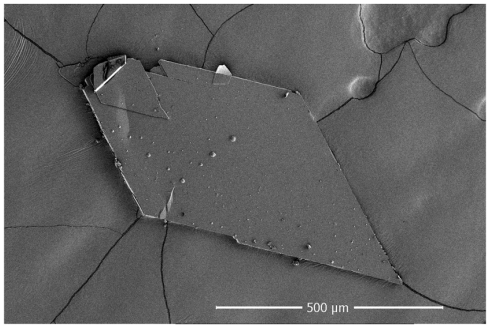

(a)

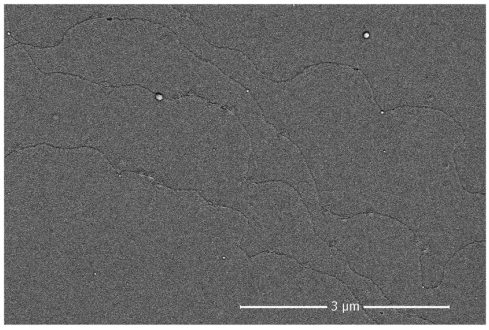

(b)

Fig. 5 (a) SEM images of a lozenge crystal of C4F3 that has been previously subjected to five consecutive cycles of transitions between phases I and II. The scale bar is 500 μm. (b) SEM image of a portion of the surface of the lozenge. The scale bar is 3 μm.

No distortion, crack or fracture is present in the SEM images of Fig. 5, even at high enhancement level. This is confirmed in the collection of SEM images of ESI, in which also the lateral faces of the crystals are scanned. The surface morphology does not show significant differences too. In both cases the surface of the crystal is compact and, at higher enhancement level, it reveals a common pattern, whose traces are evident in Figs. 4(b) and 5(b) (and in Figs. S10-S12 of ESI), suggesting a terraced morphology. The surface morphology is confirmed by the AFM measurements reported in Fig. 6 and ESI.

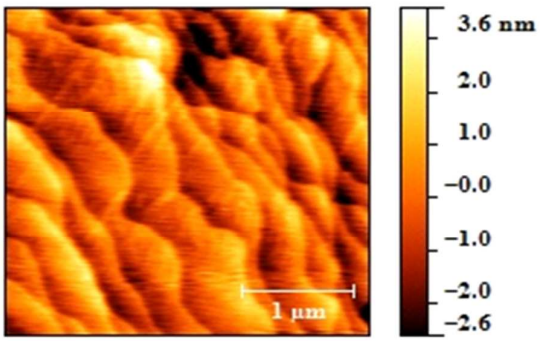

Fig. 6 AFM height image of the top of a lozenge crystal previously subjected to five cycles of transition between phases I and II. Same batch but different specimen as compared to that of Figs. 4 and 5. The scale bar is 1 μm.

In particular, the steps of the terraces are small, being only few nanometers deep.

In ESI are reported movies of the transition recorded at the optical microscope for two different single crystal specimens: under polarized light (movie1, same crystal specimen of Fig. 3) and non polarized light (movie2).

In particular, in movie1, by slowing down the rate of reproduction, it is clearly seen that the line of the front phase is very well defined: it starts at a border of the lozenge, quickly spanning the whole crystal up to the opposite border; an estimate of the linear speed of progression of the phase front (the habit plane) is 4 mm/s.[12] These features are typical of displacive diffusionless transitions.[13] In any case, looking at the movies of the SCSC transition (movies 1 and 2 in ESI) one has a strong feeling of an elastic wave propagating across the crystal. This is noteworthy if we consider that before the transition single crystals are very fragile (lozenges like that of fig. 3 must be manipulated very carefully and are easily broken in pieces by small pressure with a metal tip), while at the transition it is as if they were plastic, getting deformed without being broken or shattered. This has some resemblance with the traditional lattice-instability theories of melting.[14]

Structural characterization of the crystal polymorphs

The X-ray molecular structure of C4F3 in the phase I is shown in Fig. 7.

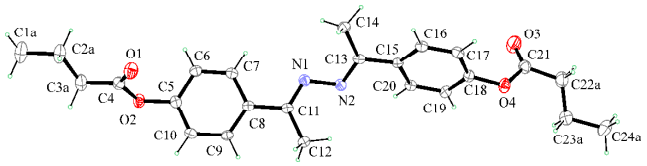

Fig. 7 ORTEP diagram of C4F3, crystal phase I at 173 K. Thermal ellipsoids are drawn at 30 % probability level. Only the most populated orientation of the disordered alkyl tails is shown.

The two phenyl rings are not coplanar, making a dihedral angle of 63.31(7)°. This is achieved mainly through a torsion around the N–N bond (C11–N1–N2–C13 = -137.7(3)°). A similar result has been found in several crystal structures containing the dimethylbenzalazine moiety[15] and can be explained on the basis of the low torsional potential around the bond N–N (less than 1 kcal/mol for torsion angles between 100° and 180°).[16] It is noteworthy, however, that in the compound analogous to C4F3, but with a propanoyloxy tail (instead of butanoyloxy), the torsion angle around the bond N–N is 180° and the conformation of the dimethylbenzalazine core is nearly planar.[17] The terminal tails of the molecule are disordered over two sites; in one case the two split positions correspond to the *trans* planar conformation and to a conformation with one *gauche*-type bond (shown in Fig. 7). The conformational disorder of the tails is consistent with the packing, shown in Fig. 8.

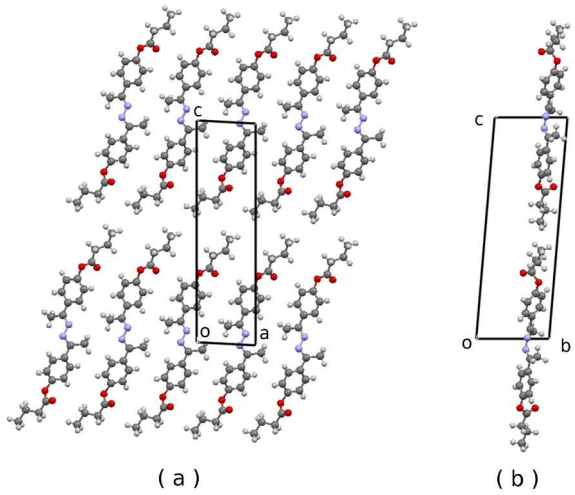

Fig. 8 C4F3, phase I. (a) A sheet of molecules viewed down b; (b) the same sheet viewed down a.

Sheets of layered molecules are formed by lattice translations in the plane (a, c). The sheets are parallel to the lattice planes (0 k 0) and have equations y=1/4 and y=3/4 (only the latter is shown in Fig. 8(b)). This implies that reflection 020 should be very strong and 010 very weak.[18] In fact, the reflection 020 is the most intense of the whole diffraction pattern. Within the sheets, molecules are layered along c with the long molecular axis tilted with respect to c; moreover, there is no interdigitation between molecules of adjacent layers. This is consistent with the thermal motion and the conformational disorder of the terminal atoms of the tails.

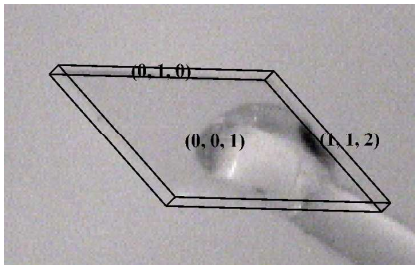

Fig. 9. Face indexing of a thin lozenge of C4F3 at 25 °C (phase I). The crystal is fastened to the tip of a glass fiber by a drop of epoxy glue.

A comparison between Fig. 8 and Fig. 9, in which the faces of a single crystal of C4F3 are indexed, allows to deduce that molecules are layered along the macroscopic direction corresponding to the thickness of the lozenges.

In Fig. 10 are reported X-Ray rotation photographs of a single crystal of C4F3 at 25 °C (phase I) and at 95 °C (phase II).

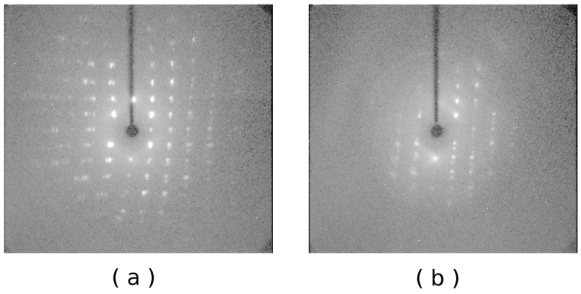

Fig. 10. X-Ray rotation photographs of a single crystal of C4F3 (MoKα). The rotation axis is b. (a) T = 25 °C, phase I; (b) T = 95 °C, phase II. The same crystal, rotation angle and exposure time was used in photographs (a) and (b).

Although the nature of single crystal is substantially preserved during the transition, the quality of the diffraction pattern of the high temperature polymorph is poorer and is characterized by a strong reduction of the number of reflections, in particular in the high sinθ/λ region. Actually, no reflection beyond θ = 16° was recorded with MoKα radiation even for large crystals and long exposure times. This, of course, can prevent the solution of the crystal structure by direct methods that, in fact, failed. The diffraction pattern of the high temperature polymorph was indexed according to a triclinic cell similar to the cell of polymorph I. In Table 1, the cell parameters are given for the two polymorphs.

Table 1. Cell parameters of the two polymorphs of C4F3.

Phase	a (Å)	b (Å)	c (Å)	α (°)	β (°)	γ (°)
I[a]	6.266(1)	7.749(1)	23.654(7)	94.58(2)	92.72(2)	93.35(5)
II[b]	6.331(1)	8.375(1)	23.202(7)	99.34(2)	85.61(2)	94.23(1)

a: measured at 25 °C; b: measured at 95 °C.

In Fig. 11 is reported the volume of the unit cell as a function of the temperature. The volume was determined from the cell parameters measured for the same single crystal at different temperature on the kappaCCD diffractometer. The sudden change of volume at the transition ($\Delta V \cong 40$ Å^3) is evident.

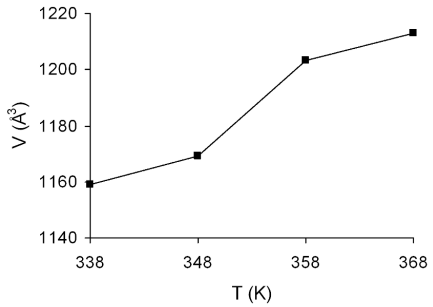

Fig. 11 Volume of the unit cell of C4F3 measured at different temperatures. The line is only a guide for the eye.

The diffraction patterns of Fig. 10 indicate that the high temperature phase of C4F3 is a disordered one. In the absence of a complete structural determination we can only discuss some hypotheses on the structural features of phase II. A possibility is that the transition involves a strong conformational disordering of the terminal alkyl chains. This hypothesis, however, can be accepted only in part. In fact, the enthalpy of fusion *per*

methylene group in compounds containing long alkyl chains is 0.98 kcal/mol.[19] That would yield, for C4F3, a value of 16.4 kJ/mol, well higher than the experimental value. So the alkyl tails of C4F3 in phase II are not liquid-like but keep a significant degree of order.[8] Another perhaps significant observation is that the reflection 020, the most intense in the diffraction pattern of phase I, has low relative intensity in the diffraction pattern of phase II. With reference to Fig. 8(b), this can suggest that in phase II molecules are tilted with respect to the planes (0k0). Moreover, molecules could be tilted in different symmetric orientations with subsequent static disorder. This picture would also be consistent with the shortening of the c axis (and enlargement of b axis) in phase II (see Table 1). From that shortening, one could estimate the tilt angle of the long molecular axis (in the plane bc) with respect to the planes (0k0) as ± 11°.

Experimental Part

Materials and methods. Differential scanning calorimetric analysis was performed with a Perkin Elmer Pyris instrument under flowing N_2, at 10 K/min scanning rate. Transition temperatures were taken at peak onset.[10b] Temperature controlled optical microscopy was performed with a Zeiss Axioskop polarizing microscope equipped with a Mettler FP90 heating stage. ^{1}H-NMR spectra were recorded with a Varian spectrometer operating at 200 MHz. SEM micrographs of single crystals of C4F3 were recorded on a FESEM FEI Nova NanoSEM 450. Crystals were deposited on a carbon tape and sputtered with a DentonVacuum Desk V HP using a Gold/Palladium target. Atomic force microscopy (AFM) height images have been obtained operating in tapping mode at room temperature with a Veeco Caliber microscope using standard silicon cantilevers TESP-MT and a resonant frequency and force constant of about 350 kHz and 50 Nm^{-1}, respectively.

Synthesis. C4F3 was prepared by reaction of 4,4'dihydroxy-α,α'-dimethylbenzalazine with butanoyl chloride in chloroform/pyridine mixture (1/1 by volume), according to the recipe given in ref. 8. The raw product was purified by column chromatography (silicagel plus chloroform as eluent). Final recystallization was performed by cooling to 4 °C a boiling ethanol solution of the product. δ_H (200 MHz; $CDCl_3$, 25 °C) 1.07 (6 H, tr), 1.82 (4 H, m), 2.41 (6 H, s), 2.56 (4 H, tr), 7.18 (4 H, d, ^3J = 8.8 Hz), 7.99 (4 H, d, ^3J = 8.8 Hz) ppm. Single crystals, in the form of thin lozenges, were obtained by slow evaporation from different solvents or solvent mixtures. In particular, the lozenges shown in Figs 3-6 and in the movies 1 and 2 were obtained from chloroform/hexane. The crystal whose diffraction pattern is shown in Fig. 10 was obtained from ethanol.

X-Ray analysis. All data for the crystal structure analysis were measured on a Bruker-Nonius KappaCCD diffractometer, equipped with Oxford Cryostream 700 apparatus, using graphite monochromated MoKα radiation (0.71073 Å), at variable temperatures. Reduction of data and semiempirical absorption correction were done using the SADABS program.[20] The structure was solved by direct methods (SIR97 program[21]) and refined by the full-matrix least-squares method on F^2 using the SHELXL-97 program[22] with the aid of the WinGX[23] software. Crystal, collection and refinement data are given in Table 2. Non-hydrogen atoms were refined anisotropically; H atoms were determined stereochemically and refined by the riding model. For all H atoms, the isotropic displacement parameter was not refined but set equal to 1.2 times the equivalent isotropic displacement parameter of the carrier atom (1.5 in the case of methyl H atoms). The analysis of the crystal packing was performed using the program Mercury.[24]

Table 2. Crystal, collection and refinement data for C4F3 (phase I)

	C4F3
Empirical formula	$C_{24}H_{28}N_2O_4$
M	408.48
System	triclinic
Space group	P-1
a /Å	6.1550(19)
b / Å	7.6400(18)
c / Å	23.508(7)
α /°	96.36(3)
β / °	91.92(3)
γ /°	94.01(3)
V / Å^3	1095.0(5)
Z	2
T / K	173
ρ_{calc} /g·cm^{-3}	1.239
Reflns collected	8814
Unique reflns (Rint)	4382 (0.0404)
R1 [I > 2σ(I)]	0.0629
wR2 [all data]	0.1905
Max. peak/ hole (e·Å^{-3})	0.309, -0.330

Conclusions

We have reported on a rare case of single-crystal-to-single-crystal transition in a compound that also exhibits a nematic liquid crystalline phase before the transition to the isotropic liquid. The transition between the two crystal phases is thermotropic and reversible. In DSC analysis, the solid-solid transition and the isotropic liquid to nematic transition are characterized by a small supercooling as compared with the nematic to crystal transition. Remarkably, the transition can be performed on the same single crystal several times, without damage of the crystal and substantial change of the surface morphology, as we have demonstrated by advanced microscopy techniques (SEM and AFM). The low temperature crystal phase has a layered structure. The crystal phase stable at higher temperature is disordered: the transition probably involves a partial orientational disordering of the molecules within the layers.

Acknowledgements

We thank the CRdC NTAP of Regione Campania (Italy) for X-Ray facility, Dr. E. Di Pace of ITPR-CNR of Naples for technical assistance in recording the movies and Dr. Rocco Di Girolamo of the University of Naples "Federico II" for AFM measurements.

Notes and references

[a] *Department of Chemical Sciences, University of Naples "Federico II", Via Cinthia, I-80126 Naples, Italy. E-mail: roberto.centore@unina.it*
[b] *Department of Chemical Engineering, Materials and Industrial Production, University of Naples "Federico II", Piazzale Tecchio, I-80125 Naples, Italy.*

† Electronic Supplementary Information (ESI) available: Movies of the single-crystal-to-single-crystal transition (heating and cooling cycle in sequence) for two different single crystals: movie1 (polarized light),

movie2 (non polarized light). Crystallographic data in CIF format for the single crystal X-ray structure of the studied compound. Collection of SEM and AFM images of a single crystal of C4F3 as prepared, and of a single crystal of C4F3 of the same batch after five consecutive cycles of transitions between phases I and II. CCDC reference number 1054627. See DOI: 10.1039/b000000x/

1 J. Bernstein, *Cryst. Growth Des.*, 2011, **11**, 632-650.

2 A. F. Wells, *Structural Inorganic Chemistry*, Clarendon Press: Oxford, 1984.

3 (a) S. L. Price, *Acta Crystallogr.*, 2013, **B69**, 313-328. (b) R. Centore, M. Causà, F. Cerciello, F. Capone and S. Fusco, *CrystEngComm*, 2014, **16**, 9168-9175.

4 (a) S. Khoshkhoo and J. Anwar, *J. Phys. D: Appl. Phys.*, 1993, **26**, B90-B93. (b) P. Rizzo, A. R. Albunia and G. Guerra, *Polymer*, 2005, **46**, 9549-9554. (c) J. Chen, M. Shao, K. Xiao, A. J. Rondinone, Y.-L. Loo, P. R. C. Kent, B. G. Sumpter, D. Li, J. K. Keum, P. J. Diemer, J. E. Anthony, O. D. Jurchescu and J. Huang, *Nanoscale*, 2014, **6**, 449-456.

5 R. D. Shannon and R. C. Rossi, *Nature*, 1964, **202**, 1000-1001.

6 IUPAC, *Compendium of Chemical Terminology*, 2nd Ed. (the "Gold Book"). Compiled by A. D. McNaught and A. Wilkinson, Blackwell Scientific Publications, Oxford, 1997.

7 (a) Ž. Skoko, S. Zamir, P. Naumov and J. Bernstein, *J. Am. Chem. Soc.*, 2010, **132**, 14191-14202. (b) R. Centore, M. Jazbinsek, A. Tuzi, A. Roviello, A. Capobianco and A. Peluso, *CrystEngComm*, 2012, **14**, 2645-2653. (c) N. K. Nath, M. K. Panda, S. C. Sahoo and P. Naumov, *CrystEngComm*, 2014, **16**, 1850-1858.

8 A. Roviello and A. Sirigu, *Mol. Cryst. Liq. Cryst.*, 1976, **33**, 19-34.

9 (a) A. Roviello and A. Sirigu, *J. Polymer Sci. Polymer Lett. Ed.*, 1975, **13**, 455-463; (b) A. Roviello and A. Sirigu, *Gazz. Chim. Ital.*, 1980, **110**, 403-406. (c) A. Roviello, S. Santagata and A. Sirigu, *Makromol. Chem. Rapid Commun.*, 1983, **4**, 281-284. (d) U. Caruso, R. Centore, A. Roviello and A. Sirigu, *Macromolecules*, 1992, **25**, 2290-2293. (e) R. Centore, B. Panunzi, A. Roviello, A. Sirigu and P. Villano, *J. Polymer Sci. Part A: Polymer Chem.*, 1996, **34**, 3203-3211.

10 (a) G. A. Oweimreen and M. A. Morsy, *Thermochim. Acta*, 1999, **325**, 111-118; (b) H. K. Cammenga, K. Gehrich and S. M. Sarge, *Thermochim. Acta*, 2006, **446**, 36-40; (c) A. Nesrullajev and N. Avci, *Mater. Chem. Phys.*, 2011, **131**, 455-461.

11 D. Demus and L. Richter, *Textures of liquid crystals*, 1978, Weinheim: Verlag Chemie.

12 Looking at the reverse transition in movie1, it is very intriguing to note that the line of the front phase moves exactly in the opposite direction as compared with the direct transition. This feature, that can be considered a macroscopic evidence of microscopic reversibility, well accounts for the nickname "military transitions" given to SCSC transformations.

13 J. W. Christian, *The Theory of Transformations in Metals and Alloys* (Pergamon, Oxford, 2002), 3rd ed.

14 (a) F. A. Lindemann, *Z. Phys.*, 1910, **11**, 609-615. (b) M. Born, *J. Chem. Phys.*, 1939, **7**, 591-603. (c) D. C. Wallace, *Proc. R. Soc. Lond. A*, 1991, **433**, 631-661.

15 (a) R. Centore, M. R. Ciajolo, A. Roviello, A. Sirigu and A. Tuzi, *Mol. Cryst. Liq. Cryst.*, 1990, **185**, 99-108. (b) R. Centore, M. R. Ciajolo and A. Tuzi, *Mol. Cryst. Liq. Cryst.*, 1993, **237**, 185-191. (c) R. Centore, A. Roviello, A. Tuzi and A. Sirigu, *Liq. Cryst.*, 2006, **33**, 929-933.

16 R. Centore and C. Garzillo, *J. Chem. Soc. Perkin Trans. 2*, 1997, 79-84.

17 M. R. Ciajolo, A. Sirigu and A. Tuzi, *Acta Crystallogr.*, 1985, **C41**, 483-485.

18 If the atoms strictly belonged to the planes y = 1/4 and y = 3/4, then the expression of the structure factor for reflections 010 and 020 would be: $F_{010} = \exp(i\pi/2)\cdot(\sum f_j) + \exp(i\pi 3/2)\cdot(\sum f_j) = i(\sum f_j) - i(\sum f_j) = 0$ and $F_{020} = \exp(i\pi)(\sum f_j) + \exp(i\pi 3)(\sum f_j) = -(\sum f_j) - (\sum f_j) = -2(\sum f_j)$.

19 M. Dvolaitsky, F. Poldy and C. Taupin, *Physics Lett.*, 1973, **45A**, 454-456.

20 Bruker-Nonius (2002) SADABS, Bruker-Nonius, Delft, The Netherlands.

21 A. Altomare, M. C. Burla, M. Camalli, G. L. Cascarano, C. Giacovazzo, A. Guagliardi G. G. Moliterni, G. Polidori and R. Spagna, *J. Appl. Crystallogr.*, 1999, **32**, 115-119.

22 G. M. Sheldrick, *Acta Crystallogr.*, 2008, **A64**, 112-122.

23 L. J. Farrugia, *J. Appl. Crystallogr.*, 2012, 45, 849-854.

24 C. F. Macrae, I. J. Bruno, J. A. Chisholm, P. R. Edgington, P. McCabe, E. Pidcock, L. Rodriguez-Monge, R. Taylor, J. van de Streek and P. A. Wood, *J. Appl. Cryst.*, 2008, **41**, 466-470.

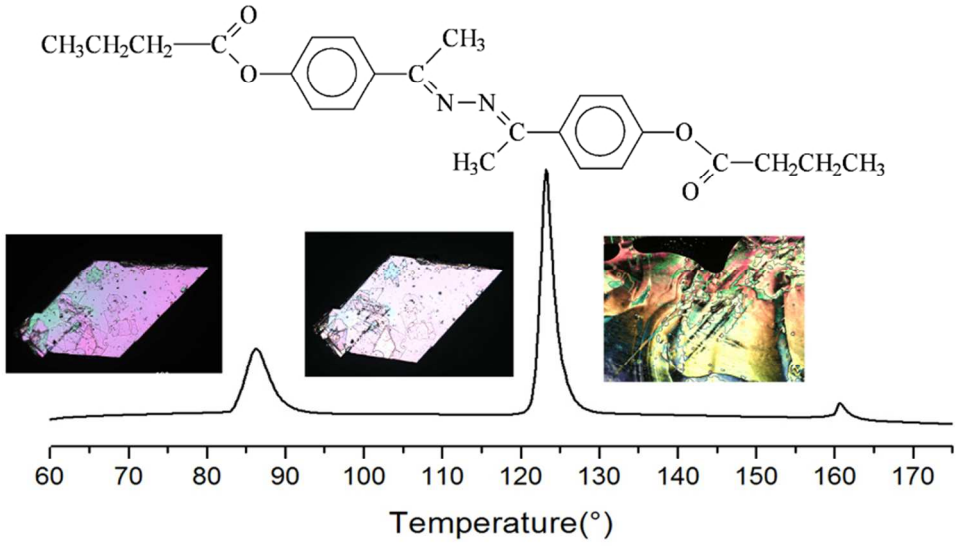

The title compound has two crystal phases related by an enatiotropic single-crystal-to-single-crystal transition and a nematic liquid crystalline phase before the isotropic liquid phase.
80x45mm (300 x 300 DPI)